International Journal of Nanomedicine

Dovepress
open access to scientific and medical research

Open Access Full Text Article

ORIGINAL RESEARCH

Interaction between immobilized polyelectrolyte complex nanoparticles and human mesenchymal stromal cells

This article was published in the following Dove Press journal:
International Journal of Nanomedicine
8 May 2014
Number of times this article has been viewed

Beatrice Woltmann[1]
Bernhard Torger[2,3]
Martin Müller[2,3,*]
Ute Hempel[1,*]

[1]Dresden University of Technology, Faculty of Medicine Carl Gustav Carus, Institute of Physiological Chemistry, Dresden, Germany; [2]Leibniz Institute of Polymer Research Dresden, Department of Polyelectrolytes and Dispersions, Dresden, Germany; [3]Dresden University of Technology, Department of Chemistry and Food Chemistry, Dresden, Germany

*These authors contributed equally to this work

Background: Implant loosening or deficient osseointegration is a major problem in patients with systemic bone diseases (eg, osteoporosis). For this reason, the stimulation of the regional cell population by local and sustained drug delivery at the bone/implant interface to induce the formation of a mechanical stable bone is promising. The purpose of this study was to investigate the interaction of polymer-based nanoparticles with human bone marrow-derived cells, considering nanoparticles' composition and surface net charge.

Materials and methods: Polyelectrolyte complex nanoparticles (PECNPs) composed of the polycations poly(ethyleneimine) (PEI), poly(*L*-lysine) (PLL), or (*N*,*N*-diethylamino)ethyldextran (DEAE) in combination with the polyanions dextran sulfate (DS) or cellulose sulfate (CS) were prepared. PECNPs' physicochemical properties (size, net charge) were characterized by dynamic light scattering and particle charge detector measurements. Biocompatibility was investigated using human mesenchymal stromal cells (hMSCs) cultured on immobilized PECNP films (5–50 nmol·cm^{-2}) by analysis for metabolic activity of hMSCs in dependence of PECNP surface concentration by MTS (3-[4,5-dimethylthiazol-2-yl]-5-[3-carboxymethoxyphenyl]-2-[4-sulfophenyl]-2H-tetrazolium, inner salt) assay, as well as cell morphology (phase contrast microscopy).

Results: PECNPs ranging between ~50 nm and 150 nm were prepared. By varying the ratio of polycations and polyanions, PECNPs with a slightly positive (PEC^{+}NP) or negative (PEC^{-}NP) net charge were obtained. The PECNP composition significantly affected cell morphology and metabolic activity, whereas the net charge had a negligible influence. Therefore, we classified PECNPs into "variant systems" featuring a significant dose dependency of metabolic activity (DEAE/CS, PEI/DS) and "invariant systems" lacking such a dependency (DEAE/DS, PEI/CS). Immunofluorescence imaging of fluorescein isothiocyanate isomer I (FITC)-labeled PECNPs suggested internalization into hMSCs remaining stable for 8 days.

Conclusion: Our study demonstrated that PECNP composition affects hMSC behavior. In particular, the PEI/CS system showed biocompatibility in a wide concentration range, representing a suitable system for local drug delivery from PECNP-functionalized bone substitute materials.

Keywords: mesenchymal stromal cells, biocompatibility, morphology, MTS assay, polyelectrolyte complex nanoparticles

Correspondence: Martin Müller
Leibniz Institute of Polymer Research Dresden, Department of Polyelectrolytes and Dispersions, Hohe Strasse 6, 01069 Dresden, Germany
Tel +49 351 465 8405
Fax +49 351 465 8231
Email mamuller@ipfdd.de

Ute Hempel
Dresden University of Technology, Faculty of Medicine Carl Gustav Carus, Institute of Physiological Chemistry, Fetscherstrasse 74, 01307 Dresden, Germany
Tel +49 351 458 6430
Fax +49 351 458 6317
Email hempel-u@mail.zih.tu-dresden.de

Introduction

The self-repair ability of bone tissue allows for healing of small defects. Large bone defects, namely critical size defects caused by difficult fractures or osteolysis, often show impaired healing. In osteoporotic patients, the diminished bone mass and altered microarchitecture of bone results in increased fragility and susceptibility to fractures.[1–3] Fracture fixing in predestined fracture sites of those patients, such as hip and vertebrae, is a challenge for orthopedic surgeons.[4,5] Implant loosening and deficient osseointegration are frequent problems. For this purpose, materials are needed that assist and guide the healing process by mechanical and biochemical control.

In particular, bone-forming osteoblasts, which arise from mesenchymal stromal cells, should be pushed to migrate, proliferate, and differentiate in order to regenerate the defective tissue.[6,7] A strategy for this aim is the modification of common biomaterials: eg, titanium-based implants,[8–10] scaffolds, and composite materials made of biodegradable polymers, calcium phosphate-based biomaterials,[11–13] bioactive glasses,[14] and glass ceramics,[15] with bioactive molecules and therapeutic drugs that can act locally at the site of the bone defect. For a controlled release of bioactive molecules and therapeutic drugs, polymer-based nanoparticles can be used as a modification of bone substitute and replacement materials.[16,17]

In this study, we have selected polyelectrolyte complex (PEC) nanoparticles (NPs) as the polymer-based NPs. PECNPs can be prepared by controlled mixing of oppositely charged polyelectrolytes (PELs), originally established by Kabanov and Zezin[18] and later followed by Philipp et al[19] and others.[20,21] PECNPs have apparent advantages over other polymer-based NP systems concerning easy availability and preparation, usage of biorelated and water-based educts and products, and adhesiveness with bone substitute materials. Up to now, PECNPs have not been assigned to one of the nanomedicine classes denoted or defined in classical review articles like that of, for example, Duncan and Gaspar.[22] However, their potential in respect of sizing (20–500 nm), shaping (spheres, rods), and surface chemistry variation (eg, charge sign) match well with those of nanomedicines, as we pointed out in a recent review.[21]

Recently, we reported on successful loading and retarded release of the bisphosphonates pamidronate and zoledronate by the branched/linear PECNP system poly(ethyleneimine) (PEI)/cellulose sulfate (CS) from model substrates (like ATR-crystals of germanium and silicon).[23,24] Based on this work, in this study heteropolymeric PECNPs composed of the polycations PEI, poly(*L*-lysine) (PLL), or (*N,N*-diethylamino)ethyldextran (DEAE) and the polyanions dextran sulfate (DS) or CS, respectively, were immobilized and used as a substrate for human mesenchymal stromal cells (hMSCs). The investigation of these PECNPs was based on the anticipation that the combination of a branched PEL with an oppositely charged linear PEL results in PECNPs whose internal structure is more compact than branched/branched or linear/linear combinations.[21] Such compact or dense PEL particles are envisioned to show higher retention and slower release of loaded drugs. The investigated PECNPs are aimed at both release of bone therapeutic drugs and binding on relevant bone substitute materials.

The aim of this study was to identify PECNP systems that are highly biocompatible and accepted in an immobilized manner in a broad concentration range by hMSCs and to study their putative internalization. Thereby, we focused on empty PECNPs and undifferentiated hMSCs. hMSCs were cultured onto PECNP films and analyzed for metabolic activity, morphological changes, and internalization features. To the best of our knowledge, there is no report published yet on the interaction of PECNPs in the used compositions with hMSCs.

Materials and methods

Materials

CS (2,900 kDa, degree of substitution d_S=2.87) was purchased from Acros Organics (Geel, Belgium). DEAE (500 kDa) and sodium DS (500 kDa, degree of substitution d_S=2.93) was from Carl Roth GmbH & Co. KG (Karlsruhe, Germany). Fluorescein isothiocyanate isomer I (FITC)–DEAE–Dextran (DEAE–FITC) (150 kDa), FITC, PEI (750 kDa), PLL (58.9 kDa), and FITC-labeled PLL (PLL–FITC) (30–70 kDa) were purchased from Sigma-Aldrich (St Louis, MO, USA). The FITC-labeled PEI (PEI–FITC) was prepared from PEI (750 kDa) incubated with FITC, and in modification to the published protocol for PLL–FITC,[25] water was used instead of Tris buffer. The anionic sodium poly(ethylenesulfonate) and cationic poly(diallyldimethylammonium chloride) PEL solution, which were used for particle charge detector (PCD) titration, were purchased from BTG Instruments GmbH (Herrsching, Germany).

Twenty-four-well tissue culture polystyrene (TCPS) plates were purchased from Nunc A.S. (Roskilde, Denmark). α-Minimal Essential Medium (α-MEM) with nucleosides, penicillin/streptomycin (10,000 U/10,000 µg/mL), *L*-alanyl-*L*-glutamine (200 mM), and phosphate buffered saline (PBS) without Ca^{2+} or Mg^{2+} were from Biochrom AG (Berlin, Germany). Fetal calf serum was purchased from BioWest (via Th. Geyer & Co. KG, Hamburg, Germany).

Preparation of PECNPs

Polycations and polyanions were dissolved in sterile water to achieve concentrations of 2 mM related to their monomer units. As not all monomer units are necessarily charged, the true concentration of charged units (n^-, n^+) can be determined by colloid titration (see next section). Related to these charged units, PECNPs composed of n^-/n^+=0.9 (positively charged PECNPs, PEC^+NP) and n^-/n^+=1.1 (negatively charged PECNPs, PEC^-NP) were prepared by mixing respective volumes of 2 mM polycation and 2 mM polyanion solutions. To prepare PECNPs, the defined pH value settings of the respective PEL solution were used and no additional salt (ionic strength) was added. For PEC^+NP dispersions,

the polyanion solution (minority component) was dosed into the polycation (majority component) solution under moderate stirring speed (400–500 rpm), whereas for PEC–NP dispersions, it was performed in the reverse order.

Characterization of PEL solutions and PECNPs

The actual amount of charges in PEL solutions was determined by colloid titration using the PCD (BTG Instruments GmbH, Herrsching, Germany). The PCD consists of the components BTG Mütek™ PCD-T3 Titrator and PCD-04. 1 mM sodium poly(ethylenesulfonate) solution was used to titrate the polycation; 1 mM poly(diallyldimethylammonium chloride) solution was used as a standard to titrate the polyanion. Based on the titrated volume (V_{TIT}) of the respective 1 mM standard solutions, the factor F of the given PEL solution with c_{PEL}=1 mM related to monomer units and with V_{PEL}=1 mL was calculated by $F=V_{TIT}/V_{PEL}$ (mL/mL). PECNP diameters were determined by dynamic light scattering (DLS) at the Zetasizer 3000 of Malvern Instruments Ltd (Malvern, UK) equipped with an He–Ne laser with 5 mW at 632.8 nm at 25°C and a detection angle of 90°. The measurements were performed applying an automatic duration time and the automatic analysis mode. The samples were held in 10 mm cuvettes. The hydrodynamic diameter D_H was estimated using the Stokes–Einstein equation. Intensity-weighted DLS data were considered, as they were applied earlier therein.[26] Errors of D_H are related to the standard deviation of at least three different sample measurements. The Zetasizer 3000 Software (PCS v.1.61 Rev 1) of Malvern Instruments Ltd was used for recording and calculating DLS parameters.

Immobilization of PEL and PECNPs onto tissue culture polystyrene

PEL as well as PECNPs were immobilized onto TCPS plates by adding aliquots of an aqueous PEL solution or PECNP dispersion (each 2 mM) in 100 µL of sterile water (Milli-Q PF Plus water) (Millipore, Monsheim, France) to finally get 5–50 nmol·cm^{-2} PELs or PECNPs, respectively. Both, PEL solutions and PECNP dispersions were air-dried overnight under laminar flow and sterilized with ultraviolet light. Immobilized FITC-labeled PECNPs were not sterilized. The spatial distribution of PECNPs after immobilization was visualized by scanning force microscopy (SFM).

Spatial distribution of PECNPs

SFM images were recorded from PECNP films on TCPS using Nanostation II of Bruker Nano GmbH (Karlsruhe, Germany) with silicon probe tips from Nanosensors (Darmstadt, Germany) with apex radii of around 10 nm. The bottoms of the 24-well TCPS plates were carefully sawn out and placed on the SFM sample table. PECNP samples were measured in "noncontact mode" at 25°C in topography and error and phase modes, and scanning parameters were optimized by minimizing the signal in the error mode. Topographical images and surface profiles were generated from SFM raw data by either SISCANPro software (Bruker Nano GmbH) or SPIP software (Image Metrology A/S, Hørsholm, Denmark).

Isolation and cultivation of hMSCs

hMSCs were isolated from bone marrow aspirates obtained from healthy donors (average age 32±10 years) at the Bone Marrow Transplantation Center of the University Hospital Dresden (Dresden, Germany) and were characterized as described previously.[27] The donors gave informed consent (Ethic Vote No. EK71022010). The cells were not pooled and used for the experiments in passage 4–6. α-MEM with nucleosides supplemented with 10% heat-inactivated fetal calf serum, 20 U penicillin/mL, 20 µg streptomycin/mL, and 2 mM *L*-alanyl-*L*-glutamine was used as expansion medium. For the experiments, hMSCs were subcultured at a density of 5,500 cells·cm^{-2} onto 24-well TCPS plates. After 4 days, a medium change was performed.

Analysis of metabolic activity of hMSCs

Cells cultured on immobilized PEL, PECNP, and TCPS as a reference were analyzed at day 1 and day 8 after plating for metabolic activity using CellTiter 96® AQueous One Solution cell proliferation assay (MTS test; Promega Corporation, Fitchburg, WI, USA) according to the manufacturer's instructions, with a Benchmark Plus Microplate Reader (Bio-Rad Laboratories, Hercules, CA, USA).

Analysis of cell morphology

hMSCs were cultured for 8 days onto 20 nmol·cm^{-2} of immobilized PECNPs. The morphology of the cells was monitored using an Axiovert phase contrast microscope (Carl Zeiss Meditec AG, Jena, Germany). Digital images were obtained with an AxioCam HRc camera (Carl Zeiss Meditec AG) using AxioVision software version 4.6 (Carl Zeiss Meditec AG).

Fluorescence imaging of FITC–PECNPs and hMSCs

Fluorescent PECNPs (FITC–PECNP; 20 nmol·cm^{-2} on glass coverslips) were applied to evaluate the cytoskeleton

and to see whether PECNPs were internalized by hMSCs. After 8 days, hMSCs were washed gently with PBS and incubated with 4% paraformaldehyde (Merck KGaA, Darmstadt, Germany) (w/v) for 10 minutes. The cell membrane was permeabilized with 0.1% Triton X-100 (Ferak Laborat GmbH, Berlin, Germany) (w/v) in PBS for 20 minutes, and nonspecific binding sites were blocked with 1% bovine serum albumin (Carl Roth GmbH & Co. KG) (w/v) in PBS containing 0.05% Tween® 20 (SERVA Electrophoresis GmbH, Heidelberg, Germany) (w/v) for at least 10 minutes. F-actin stress fibers were stained with Alexa Fluor® 568 Phalloidin (A12380; Invitrogen, Darmstadt, Germany), diluted 1:250 in blocking buffer, for 60 minutes. Staining of hMSC nuclei was performed with 0.2 µg 4',6-diamidino-2-phenylindole (DAPI, Roche, Basel, Switzerland)/mL PBS (Sigma-Aldrich) for 15 minutes. All steps were performed at 25°C. Afterwards, hMSCs were embedded in Mowiol® 4-88 (Sigma-Aldrich) and visualized using an AxioPhot fluorescence microscope (Carl Zeiss Meditec AG). Fluorescence signals were detected using filters for Alexa Fluor® 568 Phalloidin: $\lambda_{excitation}$=578 nm and $\lambda_{emission}$=603 nm, DAPI: $\lambda_{excitation}$=365 nm and $\lambda_{emission}$=420 nm, and FITC–PECNP $\lambda_{excitation}$=490 nm and $\lambda_{emission}$=525 nm. Digital images were gained with an AxioCam MRm camera (Carl Zeiss Meditec AG) using AxioVision software version 4.6 (Carl Zeiss Meditec AG).

Statistical analysis

All data were derived from different hMSC preparations and treated as independent biological replicates. Analysis of statistical significance was performed with GraphPad Prism 5 software (Statcon, Witzenhausen, Germany) by analysis of variance (ANOVA) with Bonferroni's post-test. Two-way ANOVA was performed to compare polycations and polyanions and to analyze the impact of net charge and chemistry of the PECNPs on metabolic activity. The influence of the PEL or PECNP amount compared with TCPS was analyzed by one-way ANOVA. Two-tailed Student's *t*-test was used to analyze the difference of metabolic activity of hMSCs from day 1 to day 8 and differences amongst the PECNP systems radii dependent on the composition or PECNP net charge. The results are presented as mean ± standard error of the mean (SEM).

Results and discussion

Characterization of PECNPs

Twelve PECNP systems differing in PEL composition and net charge were prepared and characterized. Both synthetic and biorelated PELs were selected. Their combinations used for the preparation of PECNPs are listed in Table 1. The linear polycation PLL and the branched polycations PEI and DEAE were combined with the linear polyanion CS and the branched polyanion DS. By varying the molar mixing ratio n^-/n^+ of polycationic and polyanionic components, the resulting PECNP systems acquired either a slightly positive (n^-/n^+=0.9, PEC^+NP) or negative (n^-/n^+=1.1, PEC^-NP) net charge. Hydrodynamic radii (R_H) and polydispersity indices of the various PECNP systems were determined by DLS and the net charge sign$^{(\pm)}$ by the PCD, respectively. R_H values in the range between 46 nm and 146 nm were obtained for all compositions of PECNPs. In detail, PEI-containing PECNPs (PEI/DS, PEI/CS) were the smallest (R_H=46–59 nm), followed by the PLL-containing PECNPs (R_H=70–106 nm) and DEAE-containing PECNPs (R_H=103–146 nm).

Table 1 Colloid characteristics of polyelectrolyte complex nanoparticles (PECNPs)

PECNP system (abbreviation)	Mixing ratio n^-/n^+	Hydrodynamic radius (R_H) (nm)°	Polydispersity index (PDI)°	Net charge
(*N*,*N*-diethylamino)ethyldextran/ dextran sulfate (DEAE$^{¤¤¤}$/DS)	0.9	134±26†††	0.14±0.06	+
	1.1	103±20	0.15±0.07	–
(*N*,*N*-diethylamino)ethyldextran/ cellulose sulfate (DEAE/CS)	0.9	141±35	0.23±0.13	+
	1.1	146±20‡‡	0.73±0.18	–
Poly(ethylenimine)/ dextran sulfate (PEI$^{¤¤¤}$/DS)	0.9	59±16*,†††,††	0.19±0.08	+
	1.1	46±18†††	0.54±0.16	–
Poly(ethylenimine)/ cellulose sulfate (PEI/CS)	0.9	58±20‡‡‡	0.20±0.12	+
	1.1	56±16‡‡‡,‡‡	0.42±0.08	–
Poly(*L*-lysine)/dextran sulfate (PLL$^{¤¤¤}$/DS)	0.9	70±9$^{*,###,†††,††}$	0.19±0.06	+
	1.1	83±15$^{###,†††}$	0.15±0.02	–
Poly(*L*-lysine)/cellulose sulfate (PLL/CS)	0.9	106±8$^{###,‡‡‡}$	0.29±0.03	+
	1.1	97±16$^{###,‡‡‡}$	0.28±0.04	–

Notes: °R_H and PDI are calculated from ten independent measurements. Significant differences between PECNP systems with identical polycation (DEAE vs PLL vs PEI) independent of the polyanion are indicated by $^{¤¤¤}$($P<0.001$). Significant differences of positively charged vs negatively charged PECNPs of the same PECNP system are indicated with *($P<0.05$). Significant differences of PECNP systems with identical polycation and net charge vs varying polyanions are indicated by $^{###}$($P<0.001$). Significant differences of PECNP systems with identical polyanion and net charge vs varying polycations are indicated by ††($P<0.01$) and †††($P<0.001$) for DS-containing PECNP systems or ‡‡($P<0.01$) and ‡‡‡($P<0.001$) for CS-containing PECNP systems.

The particle size of the PECNPs was partially influenced by the net charge. Although DS-containing PECNPs were generally slightly smaller compared with CS-containing PECNP systems, the situation concerning the net charge was more complex. Although positively charged DEAE/DS (R_H≈135 nm; P=0.09) and PEI/DS (R_H≈60 nm; $P<0.05$) were larger than the corresponding negatively charged ones, positively charged PLL/DS (R_H≈70 nm) were significantly smaller than negatively charged PLL/DS (R_H≈80 nm; $P<0.05$). All CS-containing PECNPs, like DEAE/CS (R_H≈ 145 nm), PEI/CS (R_H≈60 nm), and PLL/CS (R_H≈100 nm), showed almost no differences in particle size for PEC^+NP compared with PEC^-NP. The polydispersity indices were ranging between 0.14 and 0.73, indicating rather broad size distributions for all PECNP systems (Table 1).

For the in vitro experiments, PECNP dispersions were immobilized on 24-well TCPS plates and thereupon incubated in buffered α-MEM cell culture medium. Due to their remarkable adhesive strength,[23,24] stable PECNP films could be generated by simple solution casting. Figure 1 shows

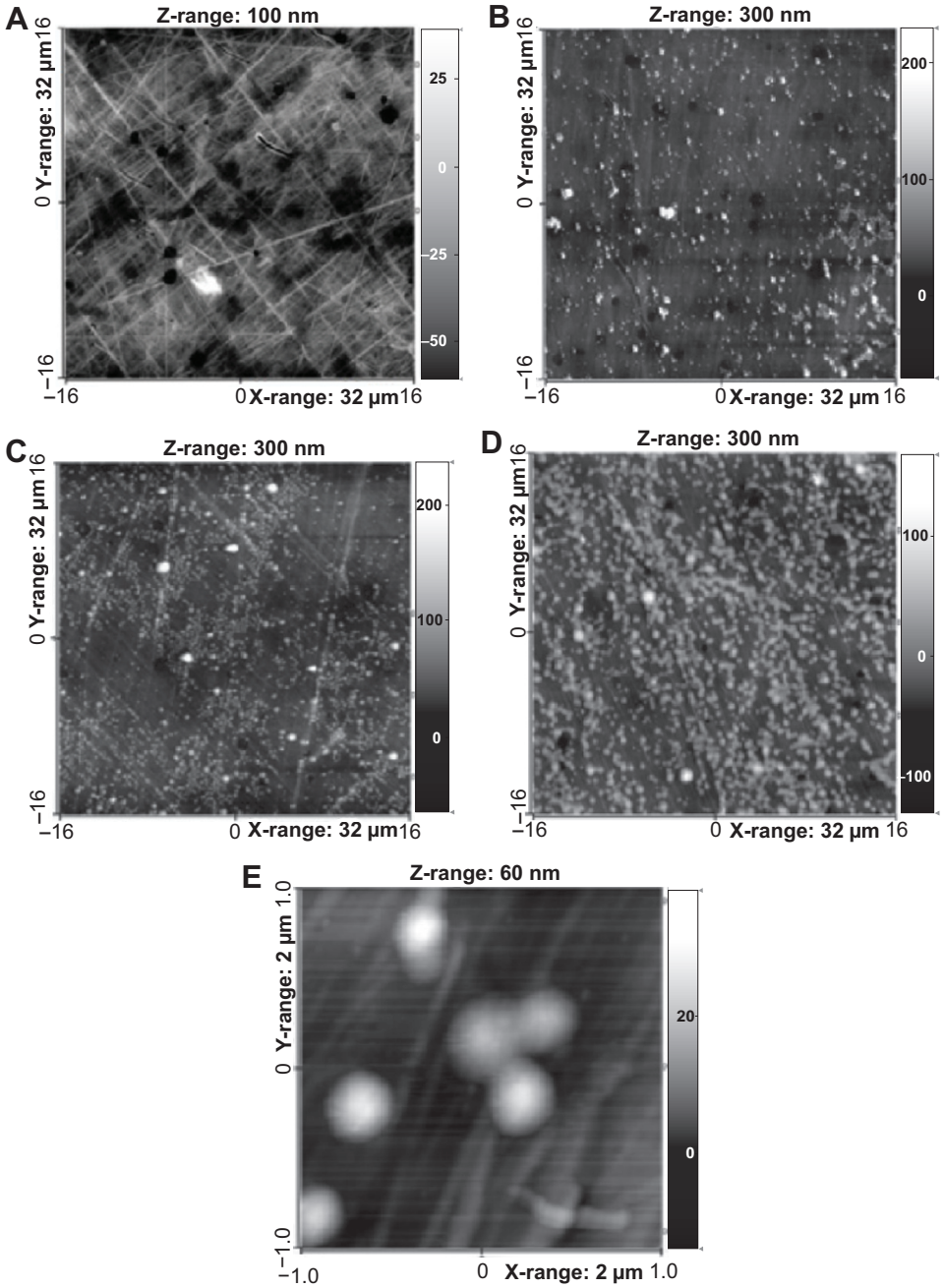

Figure 1 Scanning force microscopy (SFM) of polyelectrolyte complex nanoparticle (PECNP) films on tissue culture polystyrene (TCPS) plates.
Notes: TCPS plate (**A**) was coated with PECNPs of poly(ethyleneimine) (PEI)/dextran sulfate $(DS)^+$ at surface concentrations of 5 nmol·cm^{-2} (**B**), 20 nmol·cm^{-2} (**C**), and 50 nmol·cm^{-2} (**D**) (32 µm ×32 µm). Image (**E**) (2 µm ×2 µm) was recorded at TCPS coated with 50 nmol·cm^{-2} of PEI/DS^+.

SFM images of bare TCPS (Figure 1A) in comparison with exemplarily PEI/DS$^+$ films on TCPS (Figures 1B–D) at lower spatial resolution (32 µm ×32 µm), whereupon homogenously distributed PECNPs were seen at this scale. Importantly, with increasing initial PECNP concentration (5, 20, and 50 nmol·cm^{-2}), the density of immobilized PECNPs also increased distinctly and visibly. Finally, a higher spatial resolution SFM image (2 µm ×2 µm) of PEI/DS$^+$ at 50 nmol·cm^{-2} bound at TCPS reveals PECNPs between 50 nm and 200 nm due to a partial clustering, which is still consistent with DLS data.

Metabolic activity of hMSCs on immobilized PEL and PECNPs

To our knowledge, to date no information with regard to these PEL/PEL combinations interacting with hMSCs has been published. Solely, Tiyaboonchai et al[28] report about drug delivery from PEI/DS, and only Hartig et al[29] reported on the interaction of PECNPs in general with other cell types, in particular human microvascular endothelial cells.[30]

In this study, hMSCs were cultured on immobilized PECNP films in various surface concentrations and analyzed at day 1 and day 8 for relative metabolic activity by 3-[4,5-dimethylthiazol-2-yl]-5-[3-carboxymethoxyphenyl]-2-[4-sulfophenyl]-2H-tetrazolium, inner salt (MTS) assay. To compare the effects of PEL to uncomplexed PEL, immobilized PELs and PECNPs, respectively, in the concentration of 5–50 nmol·cm^{-2}, were used as a substrate for hMSCs. Figure 2A shows that the metabolic activity of hMSCs cultured on TCPS increased from day 1 to day 8 by about 2.8-fold. The data presented in Figures 2B–E were normalized to the metabolic activity on TCPS at day 1 (Figures 2B and 2D) and day 8 (Figures 2C and 2E), respectively. The value of 100% metabolic activity is related to untreated TCPS (Figure 2, dotted lines). In all bar plots of Figures 2B–E, the surface concentration was used as a variable.

Interaction between uncomplexed PELs and hMSCs

Figures 2B and 2C show the relative metabolic activity of hMSCs cultured on the pure PELs used in this study after 1 day (Figure 2B) and 8 days (Figure 2C). For all polycations (PEI, DEAE, PLL), a significant decrease of metabolic activity of hMSCs from 0% to 90% of TCPS in dependence of the surface concentration was seen at day 1 (Figure 2B) and from 0% to 95% compared with TCPS at day 8 (Figure 2C). At the highest surface concentration of 50 nmol·cm^{-2}, only hMSCs on PEI and DEAE showed a residual metabolic activity of 40% and 15%, respectively, at day 1. At day 8, only on PEI 25% of hMSCs remained metabolically active on this surface concentration. On the other hand, at the lowest PEL concentration of 5 nmol·cm^{-2}, tolerable values of at least 80% at day 1 and of at least 60% at day 8 were obtained for all polycations. Surprisingly, at this surface concentration, hMSCs on PEI, which is claimed to have a toxic effect on various cell lines and animals, showed almost 95% of viable cells at day 8. In that framework, Moreau et al[31] and Morgan et al[32] reported cytotoxic effects of PEI, and Hunter[33] demonstrated also the toxic effect of PEI and PLL in human cell lines. Concerning DEAE, Ebbesen[34] and Mauersberger et al[35] reported enhanced cytolysis of immune cells, L-cells, and mouse embryonic fibroblasts. Nevertheless, in our study, PEI revealed a moderate toxicity toward hMSCs, whereas PLL and DEAE displayed a higher toxic potential with increasing

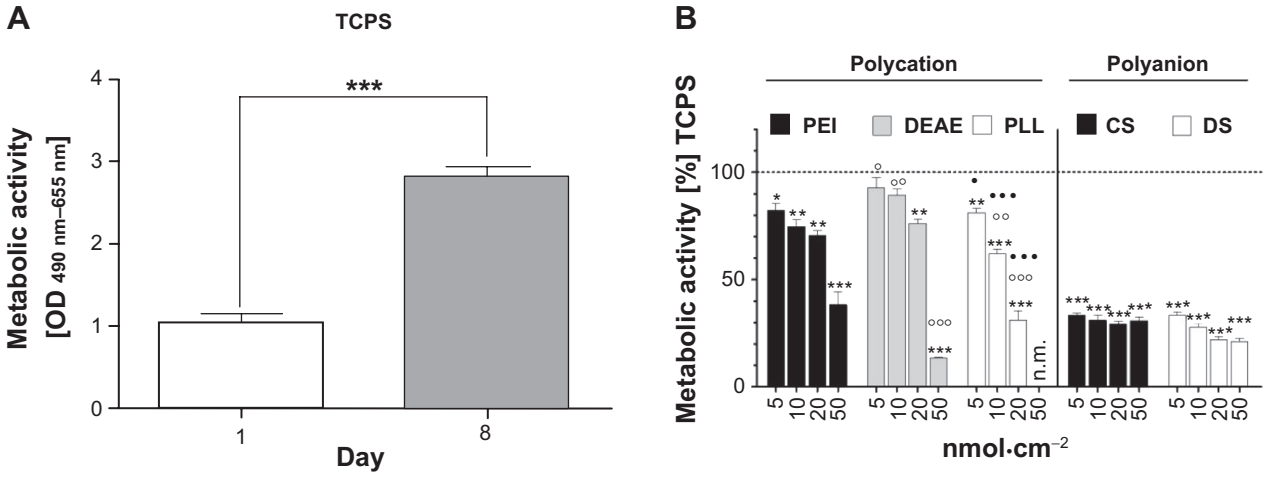

Figure 2 (*Continued*)

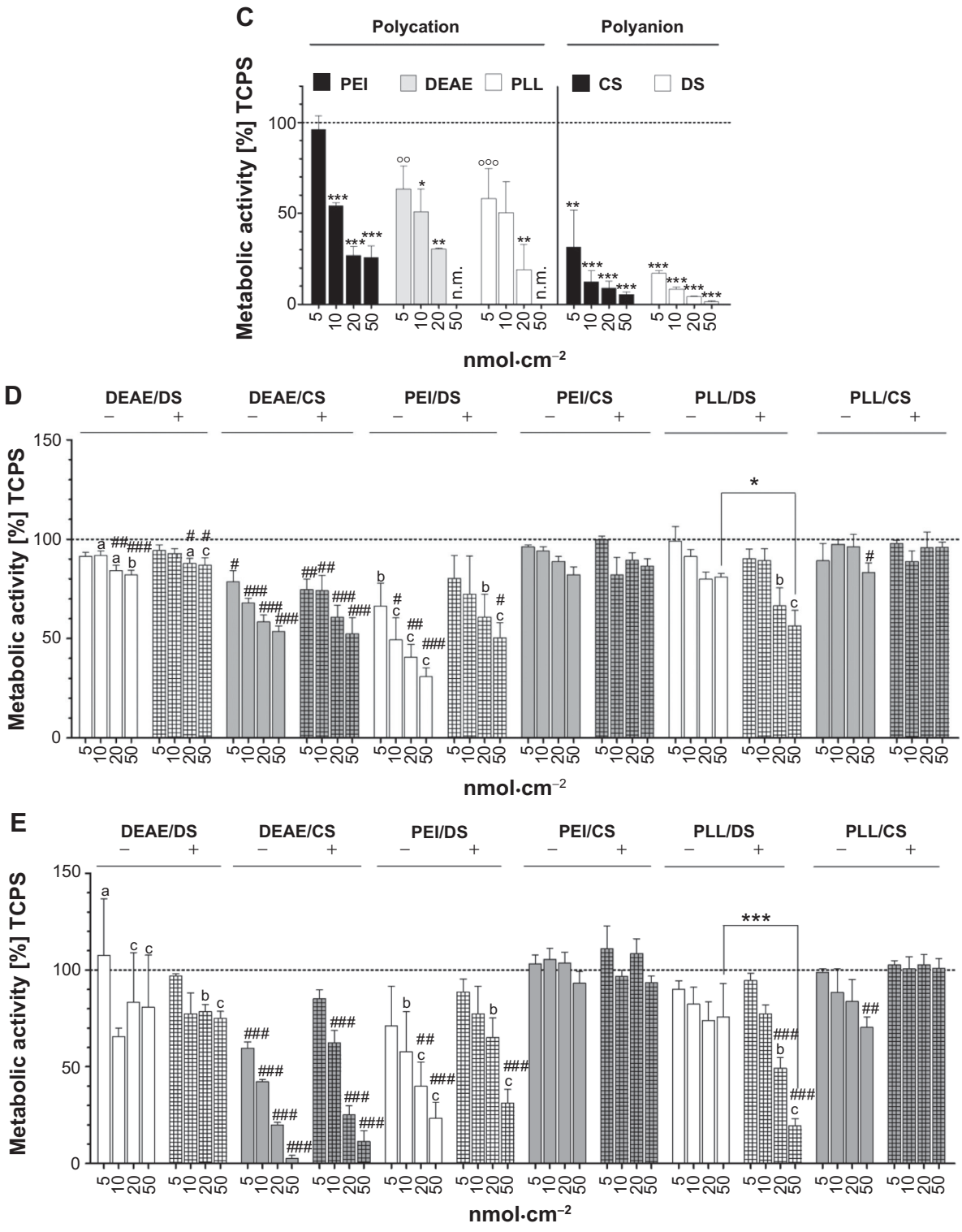

Figure 2 Metabolic activity of human mesenchymal stromal cells (hMSCs) on polyelectrolyte complex nanoparticles (PECNP) and on tissue culture polystyrene (TCPS) plates.

Notes: hMCS were cultured for 1 day (**A**,**B**,**D**) and 8 days (**A**,**C**,**E**), on TCPS (**A**) and on immobilized polyelectrolytes (PELs) (**B**,**C**) and PECNPs (**D**,**E**), and analyzed by 3-[4,5-dimethylthiazol-2-yl]-5-[3-carboxymethoxyphenyl]-2-[4-sulfophenyl]-2H-tetrazolium, inner salt (MTS) assay. Results are presented as mean ± standard error of the mean; n=3 (**A**–**C**), n=4 (**D**,**E**). Significant differences of metabolic activity of hMSCs grown on TCPS plates for 1 day vs 8 days are indicated with ***($P<0.001$) (**A**). Significant differences of PEL concentration vs TCPS of each single PEL is indicated with *($P<0.05$), **($P<0.01$), and ***($P<0.001$) (**B**,**C**). Significant differences of poly(ethyleneimine) (PEI) in the respective immobilized concentration vs the corresponding concentration of (*N*,*N*-diethylamino)ethyldextran (DEAE) or poly(*L*-lysine) (PLL) are indicated by °($P<0.05$), °°($P<0.01$), and °°°($P<0.001$) (**B**,**C**). Significant differences of DEAE vs PLL in the corresponding immobilized concentration are indicated with •($P<0.05$) and •••($P<0.001$) (**B**). Significant differences of PECNP concentration vs TCPS of each PECNP system are indicated with #($P<0.05$), ##($P<0.01$), and ###($P<0.001$) (**D**,**E**). Significant differences of positively charged vs negatively charged PECNPs of the same PECNP system are indicated with *($P<0.05$) (**D**), and ***($P<0.001$) (**E**). Significant differences of PECNP systems with identical polycation and net charge vs varying polyanions are indicated by [a]($P<0.05$), [b]($P<0.01$), and [c]($P<0.001$) (**D**,**E**).

Abbreviation: n.m., not measurable.

PEL concentrations. The overall toxic effect of uncomplexed polycations is claimed to be associated with the high charge density,[36] which is in line with reports claiming that the protonation degree influences cytotoxicity.[36,37] Further studies reported on nonphysiological effects of polycations and related them to their interaction to lipid bilayers, complexation of acidic plasma proteins, and of DNA up to agglutination and lysis of red blood cells.[29,31,38]

For the polyanion (CS, DS)-treated TCPS surfaces, the situation was even worse. Although at day 1, constant low to moderate metabolic activity around 20%–30% of TCPS was obtained for all surface concentrations (5–50 nmol·cm^{-2}), at day 8 metabolic activity decreased to 1%–30%. These results are in line with those of Kamide et al[39] reporting thrombogenicity and acute toxicity of uncomplexed CS in rats. Additionally, Hint and Richter[40] studied the treatment of rabbits with low molecular DS, which caused weight loss, cachexia, and osteoporosis.

Hence, we conclude that for uncomplexed PEI, PLL, and DEAE, only the lowest surface concentration of 5 nmol·cm^{-2} of the pure polycation-modified TCPS was tolerable at day 1. However, after 8 days of culture, only PEI modification of TCPS was well tolerated at this low concentration. CS or DS-modified TCPS even at the lowest concentration of 5 nmol·cm^{-2} was no longer tolerated by hMSCs.

Interaction between PECNPs and hMSCs

These results for TCPS modified by the uncomplexed PEL formed the basis for those obtained for TCPS modified by PECNPs, which are shown in Figure 2D (day 1) and Figure 2E (day 8). Generally, for the PECNP-modified TCPS, two types of systems could be identified. Although some of the measured PECNP systems caused a decrease of metabolic activity (DEAE/CS, PEI/DS) at day 1 and day 8, the other PECNP systems did not induce significant alterations of metabolic activity (DEAE/DS, PEI/CS) in dependence of surface concentration, respectively. The former systems were denoted as "variant systems", the latter as "invariant systems" being candidates for rather uncritical interaction between PECNPs and hMSCs. At day 8, this trend was even intensified. Interestingly, the PEL components, like PEI, DEAE, CS, and DS, used in the rather harmless "invariant systems" were found to show only low hMSC metabolic activity dependent on the surface concentration in their uncomplexed pure state. This finding is of great importance to the PECNP concept, as PECNPs, where PELs are complexed one with another, are much more compatible compared with the uncomplexed PEL used in this study. Obviously, complexation of PEL had positive effects on the biocompatibility, presumably because fewer uncompensated charges are present in the neighborhood of hMSCs.

Finally, beside the composition, also the influence of the net charge of PECNPs was studied. These systems are indicated either by the minus and plus sign in Figures 2D/E or denoted as polycation/polyanion$^{+/-}$, respectively. Obviously, the net charge itself had no effect on the response of hMSCs to PECNP systems of the same chemical composition. With the exception of PLL/DS^{+} (day 1 and 8) and PLL/CS^{-} (day 8), all variant systems remained variant and all invariant systems remained invariant in dependence of the surface concentration regardless of their net charge. This finding is very interesting, as it seems to be in contrast to those on the uncomplexed PEL. According to Figures 2B and 2C, TCPS modified by uncomplexed polyanions showed significantly less metabolic active cells compared with those on uncomplexed polycations. As an explanation, the charge argument raised here might be used, according to which the presence of too much charge reduces metabolic activity.

Complexation, regardless of whether the residual excess charges had a negative or a positive sign, significantly reduces the amount of excess charges. Thereby, it is of minor importance if this low excess charge results in PEC^{+}NP or PEC^{-}NP.

Morphology of hMSCs on immobilized PECNPs

Phase contrast microscopy images were taken to evaluate PECNP-induced morphological changes of hMSCs after 1 day and 8 days, respectively. Figure 3 shows representative images of hMSCs cultured on 20 nmol·cm^{-2} PECNPs. At day 1, after plating, hMSCs appeared as small, thin cells with typical fibroblast-like morphology; partially, hMSCs grew from cell aggregates and developed few cell–cell contacts. With the exception of PEI/DS^{-}, where the majority of the cells stayed round, on all other PECNP films a minor amount of spindle-shaped hMSCs spread and flattened to become cuboidal. Within 8 days of culture, hMSCs on TCPS and PECNP films developed filopodial extensions and formed almost confluent cell layers with fibroblast-like cuboidal hMSCs (Figure 3B). Differences in morphology were obvious when DEAE was present or when DS changed to CS (Figure 3B). An influence of the net charge was seen for PEI/DS$^{\pm}$ and PLL/DS$^{\pm}$ (Figure 3B). These morphological alterations in the presence of PECNPs confirmed MTS data. hMSCs with diminished metabolic activity in the presence of PECNPs also revealed less cell attachment and spreading (images for other PECNP concentrations are not shown). By trend, fewer hMSCs were seen on DEAE-containing PECNPs and the variant PEC systems PEI/DS$^{\pm}$ and PLL/DS$^{\pm}$ in comparison with TCPS.

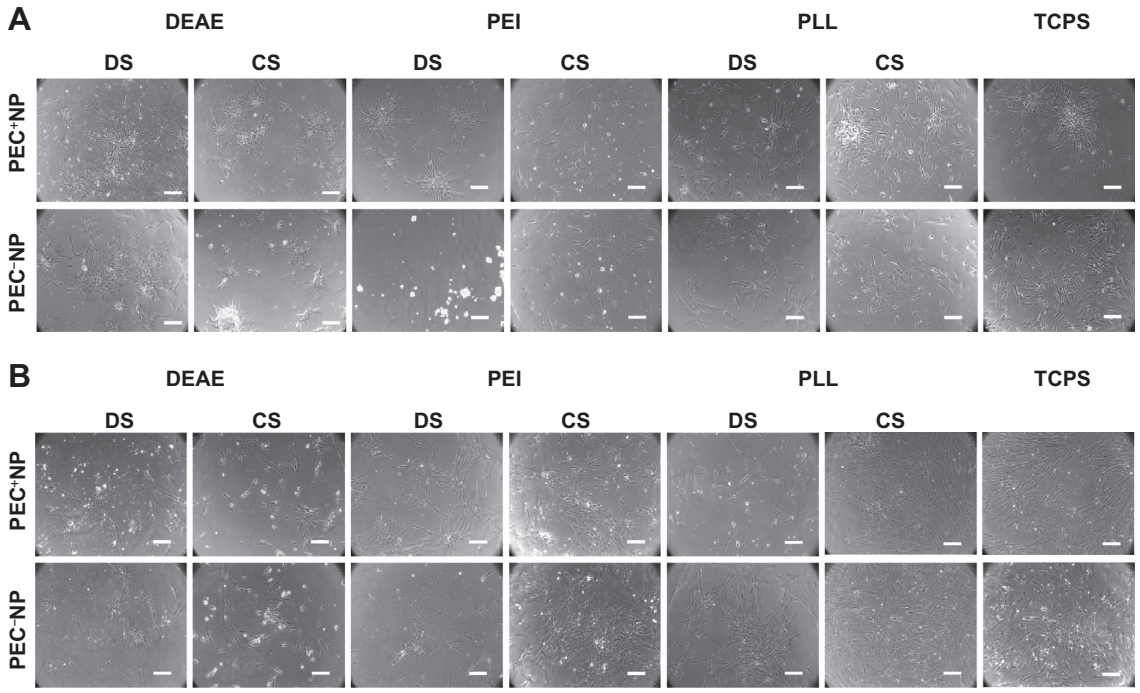

Figure 3 Morphology of human mesenchymal stromal cells (hMSCs) on polyelectrolyte complex nanoparticles (PECNPs) and on tissue culture polystyrene (TCPS).
Notes: Phase contrast micrographs of hMSCs cultured for 1 day (**A**) and 8 days (**B**) on 20 nmol·cm^{-2} PECNPs and TCPS. Scale bar 200 µm.
Abbreviations: CS, cellulose sulfate; DEAE, (*N*,*N*-diethylamino)ethyldextran; DS, dextran sulfate; PEI, poly(ethyleneimine); PLL, poly(*L*-lysine).

Fluorescence imaging of hMSCs on immobilized FITC–PECNPs

hMSCs that were cultured for 8 days on 20 nmol·cm^{-2} FITC-labelled PECNPs were analyzed for F-actin and cellular localization of the PECNPs by immunofluorescence imaging (Figure 4). The analyses were performed with PEC^{+}NPs, which were expected to feature a more efficient internalization due to their affinity for the negatively charged cell membrane.[41]

Every PECNP system displayed a well-distributed particle film on TCPS, visible as a homogeneous green background staining. An accumulation of FITC-labeled PECNPs beneath hMSCs became apparent by bright dots (see DEAE/DS and PLL/CS, Figure 4C) or areas (DEAE/CS and PEI/CS, Figure 4C). It has to be noted that the focal plane selected for these accumulated dots was situated neither at the TCPS surface below nor on top or outside of the cell body. Hence, these visible PECNPs represent a minor but considerable portion of the initial total amount of immobilized PECNPs that are located within hMSCs.

However, the question arises as to how PECNPs bound at the surface of TCPS can be internalized in cultured hMSCs. Although, generally, cellular internalization has been extensively described in the bulk phase for several nanoparticle types, depending on size, shape, surface charge, chemistry, and functionalization of the nanoparticles and also on the cell type,[42–45] cellular internalization of surface-bound nanoparticles has not been studied to that extent. Actually, we speculate that PECNPs were enclosed in the bound state by the hMSC membrane, detached, and internalized. Thus, due to the small size of PECNPs and the nonphagocytic character of hMSCs, an endocytotic mechanism is assumed.

Furthermore, hMSCs on DEAE/CS^{+} and partially DEAE/DS^{+} showed a deformation of the F-actin cytoskeleton, whereas hMSCs on other PECNP systems displayed a rather similar appearance of the cytoskeleton as seen for the TCPS control (Figure 4B), where they formed dense cell layers with tight cell–cell contacts (Figure 4A). Aggregation of PECNPs within the cytoskeleton, particularly at DEAE- and PEI-containing systems, occurred near the nucleus (Figure 4C).

Conclusively, the immunofluorescence microscopy data of Figure 4 showed that positively net charged PECNP systems were taken up by hMSCs independently of their effects on metabolic activity of hMSCs. Further microscopic and spectroscopic techniques sensitive to the distance of zones or sections in respect of the bare TCPS surface will be included in future work.

Conclusion

A set of colloidally stable and reproducible PECNP dispersions was prepared by mixing cationic PEI, PLL, or DEAE PEL with anionic CS or DS. The resulting six polycation/polyanion

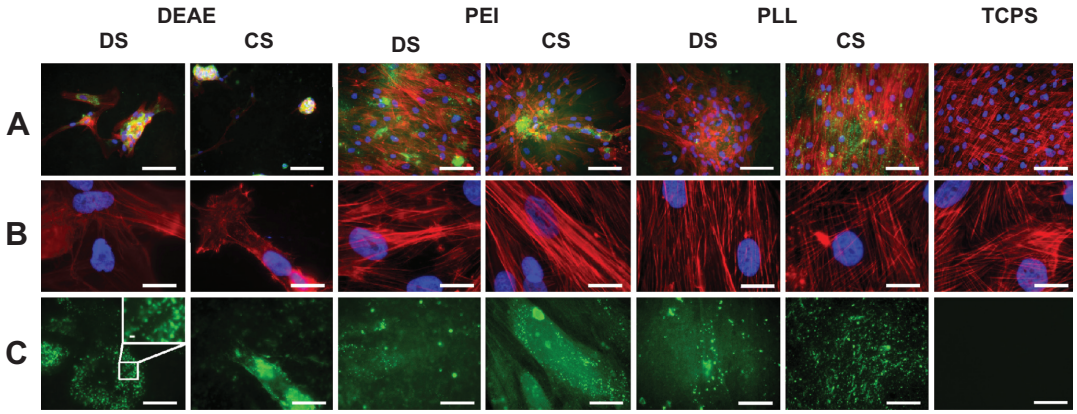

Figure 4 Detection of fluorescein isothiocyanate isomer I (FITC)-labeled polyelectrolyte complex nanoparticles with a positive net charge (PEC^+NP).
Notes: Immunofluorescence images of human mesenchymal stromal cells (hMSCs) that were cultured for 8 days on 20 nmol·cm^{-2} FITC-labeled PEC^+NP. Merged images (**A**); blue: nuclei stained with 4',6-diamidino-2-phenylindole (DAPI); red: F-actin stained with Alexa Fluor® 568 Phalloidin (**B**); green: FITC-labeled PEC^+NP (**C**). Scale bar 100 µm (**A**), 20 µm (**B**,**C**), 1 µm (**C**) (DEAE/DS zoom).
Abbreviations: CS, cellulose sulfate; DEAE, (*N*,*N*-diethylamino)ethyldextran; DS, dextran sulfate; PEI, poly(ethyleneimine); PLL, poly(*L*-lysine); TCPS, tissue culture polystyrene.

combinations possessed either a positive or a negative net charge and resulted in PECNP sizes of ~50–150 nm. PECNPs were bound in defined surface concentrations at TCPS by casting and drying their dispersions.

The PEL composition of PECNPs significantly affected metabolic activity, whereas the net charge of PECNPs did not. PECNPs could be classified into "variant systems" featuring significant surface concentration dependence on metabolic activity and "invariant systems" lacking such dependence. In particular, the PEI/CS system could be identified to show biocompatibility in a wide surface concentration range, enabling drug delivery from PECNP-functionalized biomaterials. In contrast, pure uncomplexed PEL did not show such biocompatibility at surface concentrations larger than 5 nmol·cm^{-2}. Hence, the complexation of PEL may result in a masking of their toxic properties, which supposedly is associated with charge compensation and the overall reduction of charges.

Analogous to MTS data, phase contrast microscopy revealed that the composition of PECNPs considerably affected hMSC attachment and morphology. Similar to MTS data, cell morphology on PLL/DS but also PEI/DS was influenced by PECNP net charge. Using TCPS-bound FITC–PECNPs as a fluorescent probe, it was shown that PECNPs were internalized by hMSCs and remained stable for at least 8 days. However, the uptake mechanism is still unresolved.

In future work, PECNPs will be used for the modification of bone substitute materials and the delivery of bone therapeutic drugs at the implant/bone interface in order to prevent the first-pass effect in the liver, keeping an effective drug dose, prolonging the pharmacological effects, and reducing putative side effects.

Acknowledgments

The authors want to thank Carolin Preissler and Birgit Urban for their excellent technical assistance. Human mesenchymal stromal cells were kindly provided by Professor Bornhäuser and colleagues from the Stem Cell Laboratory of Medizinische Klinik III, University Hospital Carl Gustav Carus, Dresden, Germany. This work was supported by grant of Deutsche Forschungsgemeinschaft (SFB/TR79 subprojects B4 and M7).

Disclosure

The authors report no conflicts of interest in this work.

References

1. Hayda RA, Brighton CT, Esterhai JL Jr. Pathophysiology of delayed healing. *Clin Orthop Relat Res.* 1998;355 Suppl:S31–S40.
2. Mundy GR. Pathogenesis of osteoporosis and challenges for drug delivery. *Adv Drug Deliv Rev.* 2000;42(3):165–173.
3. Kanis JA, McCloskey EV, Johansson H, Cooper C, Rizzoli R, Reginster JY. European guidance for the diagnosis and management of osteoporosis in postmenopausal women. *Osteoporos Int*. 2013; 24(1):23–57.
4. Jones CB. Augmentation of implant fixation in osteoporotic bone. *Curr Osteoporos Rep.* 2012;10(4):328–336.
5. Pesce V, Speciale D, Sammarco G, Patella S, Spinarelli A, Patella V. Surgical approach to bone healing in osteoporosis. *Clin Cases Miner Bone Metab.* 2009;6(2):131–135.
6. Granero-Moltó F, Weis JA, Miga MI, et al. Regenerative effects of transplanted mesenchymal stem cells in fracture healing. *Stem Cells.* 2009;27(8):1887–1898.
7. Neman J, Hambrecht A, Cadry C, Jandial R. Stem-cell mediated osteogenesis: therapeutic potential for bone tissue engineering. *Biologics.* 2012;6:47–57.
8. Gostin PF, Helth A, Voss A, et al. Surface treatment, corrosion behavior, and apatite-forming ability of Ti-45Nb implant alloy. *J Biomed Mater Res B Appl Biomater.* 2013;101(2):269–278.
9. Schliephake H, Bötel C, Förster A, Schwenzer B, Reichert J, Scharnweber D. Effect of oligonucleotide mediated immobilization of bone morphogenic proteins on titanium surfaces. *Biomaterials.* 2012;33(5):1315–1322.

10. Brammer KS, Choi C, Frandsen CJ, Oh S, Johnston G, Jin S. Comparative cell behavior on carbon-coated TiO2 nanotube surfaces for osteoblast vs osteo-progenitor cells. *Acta Biomater.* 2011;7(6):2697–2703.
11. Polini A, Pisignano D, Parodi M, Quarto R, Scaglione S. Osteoinduction of human mesenchymal stem cells by bioactive composite scaffolds without supplemental osteogenic growth factors. *PLoS One.* 2011;6(10):e26211. Epub 2011 Oct 12.
12. Kang Y, Scully A, Young DA, Kim S, Tsao H, Sen M. Enhanced mechanical performance and biological evaluation of PLGA coated β-TCP composite scaffold for load bearing applications. *Eur Polym J.* 2011;47(8):1569–1577.
13. Lock J, Liu H. Nanomaterials enhance osteogenic differentiation of human mesenchymal stem cells similar to a short peptide of BMP-7. *Int J Nanomedicine.* 2011;6:2769–2777.
14. Gentile P, Mattioli-Belmonte M, Chiono V, et al. Bioactive glass/polymer composite scaffolds mimicking bone tissue. *J Biomed Mater Res A.* 2012;100(10):2654–2667.
15. Chen QZ, Thompson ID, Boccaccini AR. 45S5 Bioglass®-derived glass–ceramic scaffolds for bone tissue engineering. *Biomaterials.* 2006;27(11):2414–2425.
16. Tautzenberger A, Kovtun A, Ignatius A. Nanoparticles and their potential for application in bone. *Int J Nanomedicine.* 2012;7:4545–4557.
17. Pauly S, Luttosch F, Morawski M, Haas NP, Schmidmaier G, Wildemann B. Simvastatin locally applied from a biodegradable coating of osteosynthetic implants improves fracture healing comparable to BMP-2 application. *Bone.* 2009;45(3):505–511.
18. Kabanov VA, Zezin AB. Soluble interpolymeric complexes as a new class of synthetic polyelectrolytes. *Pure Appl Chem.* 1984;56(3):343–354.
19. Philipp B, Dautzenberg H, Linow KJ, Kötz J, Dawydoff W. Polyelectrolyte complexes: recent developments and open problems. *Progr Polym Sci.* 1989;14(1):91–172.
20. Thünemann AF, Müller M, Dautzenberg H, Joanny JF, Löwen H. Polyelectrolyte complexes. *Adv Polym Sci.* 2004;166:113–171.
21. Müller M. Sizing, shaping and pharmaceutical applications of polyelectrolyte complex nanoparticles. *Adv Polym Sci.* 2014;256:197–260.
22. Duncan R, Gaspar R. Nanomedicine(s) under the microscope. *Mol Pharm.* 2011;8(6):2101–2141.
23. Torger B, Vehlow D, Urban B, Salem SR, Appelhans D, Müller M. Cast adhesive polyelectrolyte complex particle films of unmodified or maltose-modified poly(ethyleneimine) and cellulose sulphate: fabrication, film stability and retarded release of zoledronate. *Biointerphases.* 2013;8:25.
24. Müller M, Keßler B. Release of pamidronate from poly(ethyleneimine)/cellulose sulphate complex nanoparticle films: an in situ ATR-FTIR study. *J Pharm Biomed Anal.* 2012;66:183–190.
25. Bernsmann F, Richert L, Senger B, et al. Use of dopamine polymerisation to produce free-standing membranes from (PLL-HA)n exponentially growing multilayer films. *Soft Matter.* 2008;4(8):1621–1624.
26. Müller M, Keßler B, Richter S. Preparation of monomodal polyelectrolyte complex nanoparticles of PDADMAC/poly(maleic acid-alt-alpha-methylstyrene) by consecutive centrifugation. *Langmuir.* 2005;21(15):7044–7051.
27. Oswald J, Boxberger S, Jørgensen B, et al. Mesenchymal stem cells can be differentiated into endothelial cells in vitro. *Stem Cells.* 2004;22(3):377–384.
28. Tiyaboonchai W, Rodleang I, Ounaroon A. Mucoadhesive polyethylenimine-dextran sulfate nanoparticles containing *Punica granatum* peel extract as a novel sustained-release antimicrobial. *Pharm Dev Technol.* Epub 2014 Jan 17.
29. Hartig SM, Greene RR, DasGupta J, Carlesso G, Dikov MM, Prokop A, Davidson JM. Multifunctional nanoparticulate polyelectrolyte complexes. *Pharm Res.* 2007;24(12):2353–2369.
30. Hartig SM, Greene RR, Carlesso G, et al. Kinetic analysis of nanoparticulate polyelectrolyte complex interactions with endothelial cells. *Biomaterials.* 2007;28(26):3843–3855.
31. Moreau E, Domurado M, Chapon P, Vert M, Domurad D. Biocompatibility of polycations: in vitro agglutination and lysis of red blood cells and in vivo toxicity. *J Drug Target.* 2002;10(2):161–173.
32. Morgan DM, Larvin VL, Pearson JD. Biochemical characterisation of polycation-induced cytotoxicity to human vascular endothelial cells. *J Cell Sci.* 1989;94(Pt 3):553–559.
33. Hunter AC. Molecular hurdles in polyfectin design and mechanistic background to polycation induced cytotoxicity. *Adv Drug Deliv Rev.* 2006;58(14):1523–1531.
34. Ebbesen P. DEAE-dextran and polybrene cation enhancement and dextran sulfate anion inhibition of immune cytolysis. *J Immunol.* 1972;109(6):1296–1299.
35. Mauersberger B, Mickwitz CUV, Zipper J, Azt J, Heder G. Studies on cytotoxicity of poly(L-arginine), poly(L-lysine) and DEAE-dextran in L-cells and mouse embryonic fibroblasts. *Exp Pathol (Jena).* 1977;13(4–5):268–274.
36. Fischer D, Li Y, Ahlemeyer B, Krieglstein J, Kissel T. In vitro cytotoxicity testing of polycations: influence of polymer structure on cell viability and hemolysis. *Biomaterials.* 2003;24(7):1121–1131.
37. Takai T, Ohmori H. DNA transfection of mouse lymphoid cells by the combination of DEAE-dextran-mediated DNA uptake and osmotic shock procedure. *Biochim Biophys Acta.* 1990;1048(1):105–109.
38. Parhamifar L, Larsen AK, Hunter AC, Andresen TL, Moghimi SM. Polycation cytotoxicity: a delicate matter for nucleic acid therapy – focus on polyethylenimine. *Soft Matter.* 2010;6(17):4001–4009.
39. Kamide K, Okajima K, Matsui T, Ohnishi M, Kobayashi H. Roles of molecular characteristics in blood anticoagulant activity and acute toxicity of sodium cellulose sulfate. *Polym J.* 1983;15(4):309–321.
40. Hint HC, Richter AW. Chronic toxicity of dextran sulphate in rabbits. *Br J Pharmacol Chemother.* 1958;13(2):109–112.
41. He C, Hu Y, Yin L, Tang C, Yin C. Effects of particle size and surface charge on cellular uptake and biodistribution of polymeric nanoparticles. *Biomaterials.* 2010;31(13):3657–3666.
42. Zhao F, Zhao Y, Liu Y, Chang X, Chen C, Zhao Y. Cellular uptake, intracellular trafficking, and cytotoxicity of nanomaterials. *Small.* 2011;7(10):1322–1337.
43. Alexis F, Pridgen E, Molnar LK, Farokhzad OC. Factors affecting the clearance and biodistribution of polymeric nanoparticles. *Mol Pharm.* 2008;5(4):505–515.
44. Tautzenberger A, Lorenz S, Kreja L, et al. Effect of functionalized fluorescence-labelled nanoparticles on mesenchymal stem cell differentiation. *Biomaterials.* 2010;31(8):2064–2071.
45. Fröhlich E. The role of surface charge in cellular uptake and cytotoxicity of medical nanoparticles. *Int J Nanomedicine.* 2012;7:5577–5591.